Biointerface Research in Applied Chemistry
Open-Access Journal (ISSN: 2069-5837)

*Review*
**Volume 13, Issue 5, 2023, 500**
https://doi.org/10.33263/BRIAC135.500

# Radiolabeled EGFR Tyrosine Kinase for the Detection of Dual Mutations EGFR L858R/T790M in NSCLC

**Muammar Fawwaz [1,*], Mamat Pratama [1], Ainie Hasanah Aminuddin [1], Muzakkir Baits [1]**

[1] Laboratory of Pharmaceutical Chemistry, Faculty of Pharmacy, Universitas Muslim Indonesia, Makassar, Indonesia
* Correspondence: muammar.fawwaz@umi.ac.id (M.F.);

Scopus Author ID 56085116100
**Received: 28.09.2022; Accepted: 30.10.2022; Published: 6.01.2023**

**Abstract:** Non-small cell lung cancer (NSCLC) is a type of lung cancer that affects 85% of all lung cancer diagnoses. For NSCLC patients, epidermal growth factor receptor – tyrosine kinase inhibitor (EGFR-TKI) is a viable therapeutic approach. However, first- and second-generation EGFR-TKI therapies result in EGFR mutations, eventually leading to resistance. Before administering TKI therapy, the type of mutation in NSCLC must be identified in order to reduce resistance. A biopsy is a common diagnostic technique; however, a repeat biopsy in NSCLC patients is invasive. Due to the small sample size and the heterogeneous nature of cancer, the biopsy was unable to identify the mutation type accurately. The use of molecular imaging techniques such as Positron Emission Tomography (PET) and Single Photon Emission Computed Tomography (SPECT) is a promising option because it is non-invasive and can determine mutation strata in detail. Thus, this study aims to review the radiotracer developed to detect EGFR mutations, especially the double mutation EGFR L858R/T790M. Literature searches were conducted on reputable databases such as Pubmed, SciFinder, and Scopus. Our results showed that several probes were found that have high *in vitro* and *in vivo* selectivity toward double mutations EGFR L858R/T790M, such as [$^{18}$F]FEWZ, [$^{125}$I]ICO1686, [$^{77}$Br]BrCO1686, [$^{125}$I]I-osimertinib, and [$^{77}$Br]Br-osimertinib. The summary report explains that these radiotracers are insufficient to produce a high-contrast tumor in tissues. Thus, these radiotracers need to be modified by a structural modification to increase the imaging contrast of the targeted tumor for a clinical study.

**Keywords:** EGFR L858R/T790M; imaging probes; PET; SPECT; NSCLC.



## 1. Introduction

First and second-generation tyrosine kinase inhibitors (TKIs) such as gefitinib and erlotinib have been extensively developed as potent epidermal growth factor receptor (EGFR) targeted drugs [1-3]. These generations of TKI have been widely evaluated for their use in non-small cell lung cancer (NSCLC) patients [3,4]. This class of drugs can specifically bind to the intra-endothelial TK domain of EGFR and consequently block signaling pathways, thereby inhibiting tumor growth. Therefore, using these drugs is considered successful in treating cases in NSCLC [5-7]. However, treatment resistance occurs in some cases due to genetic mutations in the EGFR after several months of using first and second generations TKI [8-11].

The third-generation EGFR-TKI, osimertinib, was approved by the food drug administration (FDA) in 2015 [12]. Followed by olmutinib, which was approved for use in South Korea in 2016, and almonertinib was approved in China in 2020 [13-15]. To maximize the therapy of third-generation TKI, it is necessary to determine drug sensitivity in NSCLC

patients by detecting the type of EGFR mutation [10,16]. The diagnostic technique commonly used is the biopsy method. Gene sequencing, immunohistochemistry, and fluorescence *in situ* hybridization (FISH) analyses are frequently used in companion diagnostics following a biopsy [17-20]. However, cancer tissues are known to be heterogeneous [21,22], and a biopsy can only provide limited information on the entire cancer tissue [23]. Furthermore, patients must be burdened by recurrent intrusive biopsies [24]. Meanwhile, whole-body nuclear medicine imaging using positron emission tomography (PET) or single photon emission computed tomography (SPECT) may assess the amount of expression of a target molecule and the mutation status [25-28]. As a result, companion diagnostic imaging in nuclear medicine may be beneficial to patients.

Nuclear imaging is a diagnostic technique that is relatively safer and non-invasive than biopsy [23,29]. In addition, the nuclear imaging approach can provide complete information on the pathophysiological status and level of metastasis in cancer patients [28,30]. Positron emission tomography (PET) and single-photon emission tomography (SPECT) are two methods commonly used in nuclear imaging because of their ability to produce adequate contrast of radiotracer compounds bound to molecular targets [25,31-33].

Although PET and SPECT imaging probes targeting EGFR-TK with the L858R/T790M mutation have been developed [16,34-36], there has been little discussion of these imaging probes. This data is essential to provide an overview to future researchers regarding the optimal molecular modification technique in producing radio imaging probes that are selective for EGFR double mutations. Therefore, in this study, we aim to conduct a literature review of the results of studies that develop a selective radiotracer for EGFR L858R/T790M mutations. Several reputable databases, including Pubmed, SciFinder, and Scopus, were utilized to conduct literature searches.

This literature review was synthesized using a narrative method by grouping similar data according to the results measured to answer the objectives. Research journals that match the inclusion criteria are then collected, and a journal summary is made, including the researcher's name, the year of publication of the journal, and a summary of the results or findings. Then the summary of the research journal was entered into the table.

Our study showed that several radiotracers based on third-generation EGFR TKI were developed. However, only five targeted the double mutation EGFR L858R/T790M in NSCLC. Therefore, we described deeply the five radiotracers targeting double mutation EGFR. The types of NSCLC cells used in the articles reviewed are H1975 cells that expressed the EGFR L858R/790M mutation; H3255 and HCC827 cells expressing EGFR L858R; H441 and A549 cells expressing wild-type EGFR.

## 2. Radiolabeled on Third-Generation EGFR TKI

Third-generation EGFR TKI development focused on three critical aspects: inhibiting T790M isoform-specific kinase activity, preserving effectiveness against exon 19 and 21 mutations, and sparing inhibition of EGFR wild-type [37,38]. Osimertinib, WZ4002, EGF816, olmutinib, PF-06747775, YH5448, avitinib, and rociletinib (CO-1686) are among them [14,39]. They are effective inhibitors of T790M mutant EGFR while having little action against the wild-type receptor [39]. The covalent connection formed by these inhibitors with the C797 residue within the EGFR ATP-binding pocket is a characteristic of them [37,40]. In addition, CO-1686 promotes the formation of hydrophobic interactions with Met790 as the mutant

gatekeeper residue [4,16,35]. However, the only three that have received regulatory clearance are osimertinib, olmutinib, and almonertinib [13,14,41,42].

To successfully employ third-generation EGFR-TKIs on patients with NSCLC who have EGFR L858R/T790M mutations, PET or SPECT imaging would be a useful and non-invasive method for identifying patients who are susceptible to third-generation EGFR-TKIs. Some radiolabeled based on third-generation EGFR are provided in Table 1. This data exhibited that only four lead compounds were modified to synthesize these radiolabeled compounds, as shown in Figure 1.

**Table 1.** Radiotracer-based 3rd generation EGFR TKI.

| No. | Radiotracer | Author | Targeting |
|---|---|---|---|
| 1. | [$^{11}$C]rociletinib | Ballard *et al*., 2016 [43] | Brain exposure |
| 2. | [$^{11}$C]osimertinib | Ballard *et al*., 2016 [43] | Brain exposure |
| 3. | [$^{18}$F]FEWZ | Goggi *et al*., 2019 [34] | Imaging EGFR L858R/T790M |
| 4. | [$^{125}$I]ICO1686 | Fawwaz *et al*., 2020 [16] | Imaging EGFR L858R/T790M |
| 5. | [$^{77}$Br]BrCO1686 | Fawwaz *et al*., 2021 [35] | Imaging EGFR L858R/T790M |
| 6. | [$^{125}$I]I-osimertinib | Mishiro *et al*., 2022 [36] | Imaging EGFR L858R/T790M |
| 7. | [$^{77}$Br]Br-osimertinib | Mishiro *et al*., 2022 [36] | Imaging EGFR L858R/T790M |

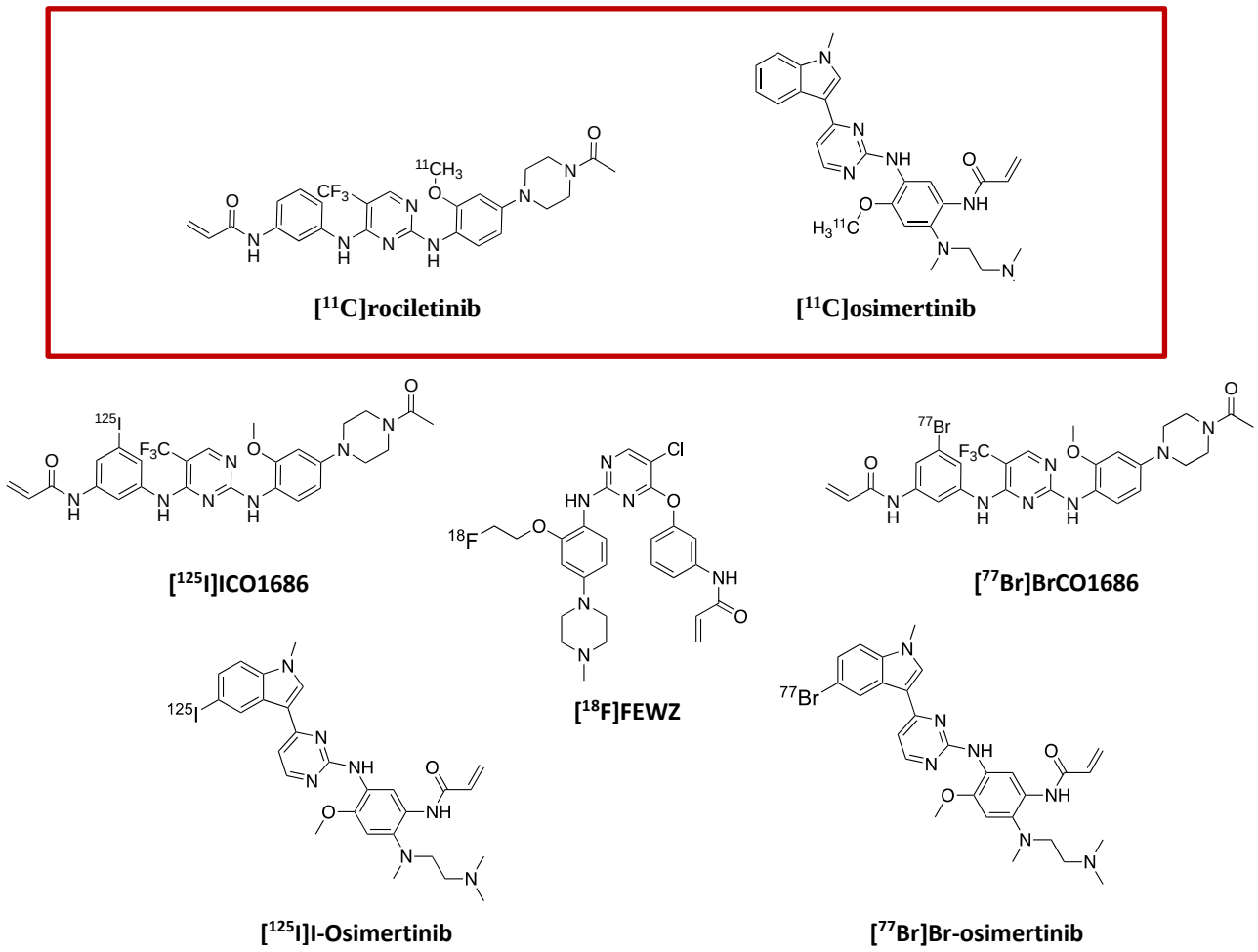


**Figure 1.** The chemical structure of radiolabeled based 3rd generation EGFR TKI.

*2.1. [$^{11}$C]rociletinib and [$^{11}$C]osimertinib.*

Ballard *et al*. reported PET imaging probes based on third-generation EGFR-TKIs, osimertinib, and rociletinib, using $^{11}$C-labeled radiotracers, [$^{11}$C]osimertinib and [$^{11}$C]rociletinib. This study assessed how well these radiotracers penetrated the brain to treat

patients with brain metastases. However, the potential of these radiotracers as imaging probes for EGFR-TK with L858R/T790M double mutations was not evaluated [43].

*2.2. [$^{18}$F]FEWZ.*

WZ4002 is the world's first third-generation TKI shown to be a strong inhibitor of T790M mutant EGFR compared to the wild-type receptor [37,44]. The radiotracer [$^{18}$F]FEWZ was synthesized by combining the WZ4002 with the molecule fluorine isotope radionuclide [$^{18}$F]. Furthermore, the purity of the [$^{18}$F]FEWZ radiotracer exceeded 97%. Three different kinds of NSCLC cells were utilized to evaluate the accumulation of [$^{18}$F]FEWZ. The studies included cytotoxicity, cell uptake, blocking assays, and radiotracer biodistribution by determination of percent injection dose per gram tissue (%ID/g) [34].

Cytotoxic evaluation of WZ4002 and [$^{19}$F]FEWZ using the cell counting kit (CCK-8) protocol with the optical density in *2-(2-methoxy-4-nitrophenyl)-3-(4-nitrophenyl)-5-(2,4-disulfophenyl)-2H* tetrazolium monosodium salt (WST-8) assay exhibited that both WZ4002 and [$^{19}$F]FEWZ have high cytotoxic effects on HCC827 and H1975 cells compared to A549 [34]. However, the addition of fluoride resulted in a slight decrease in the therapeutic effectiveness of [$^{19}$F]FEWZ, most likely owing to ethyl fluoride interfering with interactions with Leu792.

The radiotracer uptake [$^{18}$F]FEWZ on A549 was much lower than that of HCC827 and H1975 cells in the cell uptake study (Table 2). The blocking experiment, which used WZ4002 as an inhibitor, revealed a substantial reduction in radiotracer accumulation in both HCC827 and H1975 cells. In the meantime, radiotracer accumulation in A549 cells remained unchanged [34]. These results exhibited a preference uptake of radiotracer toward the mutation variant of EGFR.

**Table 2.** Assessment of [$^{18}$F]FEWZ radiotracer accumulation.

| Cell line | EGFR status | Cellular uptake (counts/well) | Biodistribution (%ID/g) | |
|---|---|---|---|---|
| | | | 5 min | 90 min |
| A549 | Wild-type | 86544 ± 7138 | 0.49 ± 0.22 | 0.58 ± 0.18 |
| HCC827 | Active mutant L858R | 231650 ± 18318 | 0.52 ± 0.25 | 0.52 ± 0.16 |
| H1975 | Dual mutation L858R/T790M | 209435 ± 13585 | 0.69 ± 0.23 | 0.90 ± 0.26 |

The biodistribution study showed that the accumulation of radiotracer in tumor H1975, was the highest of all tumors at five- and 90-minutes post-injection ($P < 0.05$) [34]. Although the accumulation of radiotracer [$^{18}$F]FEWZ was higher in the H1975 tumor, the retention value in the H1975 tumor was still relatively low at 0.90 ± 0.26% ID/g. This is because the adenosine triphosphate (ATP) binding site on EGFR is intracellular. Thus the [$^{18}$F]FEWZ must compete with high intracellular ATP concentrations for binding. Based on the evaluations above, it can be concluded that the [$^{19}$F]FEWZ radiotracer has shown some specificity to EGFR L858R/T790M. However, the overall binding is insufficient to provide contrast value by the imaging modality [34]. Thus, further studies are needed to develop the [$^{19}$F]FEWZ radiotracer to detect tumors with the EGFR L858R/T790M mutation.

*2.3. [$^{125}$I]ICO1686.*

The initial synthesis was the non-radioactive iodinated compound *N-(3-{[2-({4-[4-acetylpiperazine-1-yl]-2-methoxyphenyl}amino)-5-(trifluoromethyl)pyrimidine-4-yl]amino}-5-iodophenyl)acrylamide* (ICO1686) followed by synthesis the radioactive iodination

[$^{125}$I]ICO1686. Radiotracer [$^{125}$I]ICO1686 was synthesized using the lead compound CO-1686 labeled with an iodine isotope radionuclide in two-step reactions. The purity of the radiotracer was >99%. Three NSCLC cells, H1975, H3255, and H441, were used to evaluate the radiotracer. The assessment included cytotoxic tests, cell uptake, a blocking assay, and biodistribution.

The ICO1686 and CO-1686 revealed the cytotoxicity against EGFR L858R/T790M compared to the EGFR wild type. Although the half inhibitory concentration ($IC_{50}$) of ICO1686 was 0.31 M on EGFR L858R/T790M was weaker than that of CO-1686 ($IC_{50}$ = 0.04 M), the ICO1686 showed a higher selectivity index (SI >32) of the EGFR with the L858R/T790M double mutation than the wild type EGFR. This result is comparable to the selectivity index of CO-1686 (SI=42). Therefore, compound ICO1686 also has high specificity for EGFR L858R/T790M [16].

The cell uptake study exhibited that the accumulation of radiotracer [$^{125}$I]ICO1686 in H1975 cells was 101.52% dose/mg protein at 4 h incubation, as shown in Table 3. This value was significantly higher compared to H3255 and H441 cells. The high accumulation of radiotracer [$^{125}$I]ICO1686 in H1975 cells was due to the T790M activating mutation in the TK domain of EGFR, where T790M as a gatekeeper in the EGFR double mutation could be inhibited by the third generation of EGFR-TKI, namely CO-1686 which is the parent compound of the radiotracer [$^{125}$I]ICO1686 [16].

**Table 3.** Assessment of [$^{125}$I]ICO1686 radiotracer accumulation.

| Cell line | EGFR status | Cellular uptake (% dose/mg protein) | Biodistribution (%ID/g) | |
|---|---|---|---|---|
| | | | 1 h | 4 h |
| H441 | Wild-type | 8.95 | - | - |
| H3255 | Active mutant L858R | 33.52 | 1.63 ± 0.23 | 0.70 ± 0.13 |
| H1975 | Dual mutation L858R/T790M | 101.52 | 1.77 ± 0.43 | 0.43 ± 0.08 |

The blocking study showed that the addition of CO-1686 to H1975 cells caused a decrease in the amount of radiotracer absorption [$^{125}$I]ICO1686 from 101.52% dose/mg protein to 45.61% dose/mg protein. This indicates that the radiotracer [$^{125}$I]ICO1686 and CO-1686 compete to bind to the cells' EGFR receptor. Meanwhile, adding gefitinib did not change the amount of radiotracer absorption [$^{125}$I]ICO1686 in H1975 cells. Although H1975 cells still had the L858R mutation, adding gefitinib could not reduce the accumulation of the [$^{125}$I]ICO1686 radiotracer. This is due to the T790M mutation that inhibits the binding of gefitinib to the TK domain of EGFR, causing H1975 cells to resist gefitinib. On the other hand, adding gefitinib to H3255 cells decreases the radiotracer accumulation by more than 50% because gefitinib is the L858R EGFR-specific inhibitor [16].

Biodistribution evaluation was carried out to determine the accumulation of radiotracer [$^{125}$I]ICO1686 *in vivo*. Evaluation of the [$^{125}$I]ICO1686 was performed on normal mice and tumor carrier mice inoculated with H1975 cells and H3255 cells. Normal mice injected with radiotracer [$^{125}$I]ICO1686 were observed at 10 min, 1, 4, and 24 h. The highest accumulation was in the liver after 10 min of radiotracer injection. After 24 hours of injection, almost 70% of the radiotracer was excreted in the feces. The accumulation of the [$^{125}$I]ICO1686 in the H1975 tumor was comparable to that of the H3255 tumor [16]. These findings suggest that the nonspecific accumulation of radiotracers in the H3255 xenograft is greater than in the H1975 xenograft. Therefore, modification of this radiotracer is necessary to improve the accumulation in the targeted tumor.

*2.4. [$^{77}$Br]BrCO1686.*

The CO1686 analog was carried out by introducing bromine in the benzene ring of CO1686. Radiotracer [$^{77}$Br]BrCO1686 was synthesized starting from the non-radioactive BrCO1686. The radiotracer purity was >99%, with high stability in the phosphate buffer saline and plasma. Evaluation of the [$^{77}$Br]BrCO1686 used three NSCLC cells, namely H1975, H3255, and H441. The evaluations were carried out in cytotoxic tests, cell uptake, blocking assays, and biodistribution fields [35].

The $IC_{50}$ of BrCO1686 toward H1975 and H3255 were 0.18 M and 0.20 M, respectively. These data are comparable to that in parent compound CO1686, with the $IC_{50}$ toward H1975 and H3255 were 0.14 M and 0.15 M, respectively, indicating that the bromine substituent in the BrCO1686 does not significantly affect the activity on L858R and L858R/T790M mutated EGFR. In contrast, the cytotoxicity of the BrCO1686 against H441 cells was meaningless [35].

The cellular uptake study in Table 4 exhibited that the accumulation of [$^{77}$Br]BrCO1686 in H1975 cells was much greater than in H3255 and H441 cells. *In vitro* blocking assay with CO1686 as an inhibitor reduced radiotracer accumulation on H1975 to 56.9% dose/mg. Meanwhile, adding gefitinib as an inhibitor did not affect radiotracer accumulation in H1975 cells. However, gefitinib might reduce radiotracer accumulation in H3255 cells with the EGFR L8585R mutation [35]. The biodistribution in the normal mice revealed that the radiotracer accumulated 10 min post-injection, with the largest accumulation in the small intestine (25.38% ID/g), whose accumulation did not alter significantly 1 h post-injection [35].

**Table 4.** Assessment of [$^{77}$Br]BrCO1686 radiotracer accumulation

| Cell line | EGFR status | Cellular uptake (% dose/mg protein) | Biodistribution (%ID/g) | |
|---|---|---|---|---|
| | | | 1 h | 6 h |
| H441 | Wild-type | < 100 | 3.71 ± 0.13 | 3.30 ± 0.54 |
| H3255 | Active mutant L858R | < 100 | - | - |
| H1975 | Dual mutation L858R/T790M | 136.30 | 4.51 ± 0.17 | 3.48 ± 0.50 |

The radioactivity in the large intestine reached 47.73% ID/g 4 h post-injection. Furthermore, the accumulation of [$^{77}$Br]BrCO1686 was greater in H1975 tumors than in H441 tumors 1 h post-injection. However, compared to blood and muscle, radiotracer accumulation in the L858R/T790M tumor was insufficient. As a result, producing appropriate contrast via imaging modalities is difficult [35].

*2.5. [$^{125}$I]I-osimertinib.*

Radiotracer [$^{125}$I]I-osimertinib was synthesized from the parent compound Osimertinib. Osimertinib is a third-generation kinase inhibitor that the FDA has approved for use by NSCLC patients. The osimertinib analog was carried out by introducing iodine at an indole ring in Osimertinib [36]. The radiosynthesis obtained high purity and high stability of radiotracer. Evaluation of *in vitro* uptake study showed a high activity of radiotracer in H1975 and H3255 cells, which represents the dual mutations of EGFR. Meanwhile, the activity in H441 cells was low [36].

Evaluation of the biodistribution study showed the limited gastric absorption of [$^{125}$I]I-osimertinib suggests that *in vivo* deiodination of [$^{125}$I]I-osimertinib practically ever occurs since free iodine ions considerably accumulate in the stomach. It is well known that free iodine ions also accumulate significantly in the thyroid. The thyroid, however, was not resected in this

investigation because they anticipated that accumulation in the stomach would be a valid indicator of deiodination [36]. Table 5 exhibited that the radiotracer accumulation in H1975 was higher than H3255 at 1 h post-injection. However, radiotracer retention toward H3255 was higher than H1975 at 4 h post-injection. Furthermore, *in vivo* blocking evaluation with osimertinib reduced radiotracer accumulation on H1975 tumor significantly ($P < 0.05$). Meanwhile, adding osimertinib as an inhibitor did not affect radiotracer accumulation in H3255 tumor. Radiotracer accumulation in L858R/T790M tumor was dominant compared to blood and muscle. Thus, it is possible to produce adequate contrast by SPECT imaging modality. However, the accumulation of [$^{125}$I]I-osimertinib in the lung was much higher than in the tumor [36]. As a result, the visibility of tumors in NSCLC patients must be limited in clinical practice.

**Table 5.** Assessment of [$^{125}$I]I-osimertinib radiotracer accumulation

| Cell line | EGFR status | Biodistribution (%ID/g) | | |
|---|---|---|---|---|
| | | 1 h | 4 h | 24 h |
| H441 | Wild-type | - | - | - |
| H3255 | Active mutant L858R | 1.73 ± 0.30 | 2.93 ± 0.11 | 1.90 ± 0.65 |
| H1975 | Dual mutation L858R/T790M | 2.04 ± 0.25 | 1.97 ± 0.30 | 0.84 ± 0.27 |

*2.6. [$^{77}$Br]Br-osimertinib.*

Br-Osimertinib was developed by adding a bromine atom at the 5-position of the indole group in osimertinib. 5-fluoro-2-nitrophenol and 5-bromoindole were used as starting reagents for synthesizing Br-Osimertinib in six stages. Tributylstannyl osimertinib was produced as a radiolabeling precursor in a palladium-catalyzed cross-coupling procedure with a 6.4% yield [36].

The WST cell viability and kinase inhibition experiments indicated that Br-Osimertinib has substantial *in vitro* efficacy against the H1975 corresponded to L858R/T790M EGFR but is much less active against the wild-type EGFR. This finding supports the hypothesis that halogenation at the 5-position of the indole does not affect osimertinib's affinity for the EGFR. In enzymatic studies, Br-Osimertinib exhibited excellent selectivity for the L858R/T790M double mutations; however, in cell viability assays, they appeared to show superior selectivity against H3255 with the L858R single mutation [36].

The radiolabeling was done with carrier-free radionuclides and with no carrier added. The radiolabeled molecules and their tributylstannyl precursor were entirely isolated by HPLC purification. The radiosynthesis results obtained high purity with high stability in the phosphate buffer saline [36].

The biodistribution study toward normal mice showed that *in vivo* debromination of [$^{77}$Br]Br-osimertinib scarcely ever happens, according to organ accumulation. However, [$^{77}$Br]Br-osimertinib clearance in the blood is slow. As a result, [$^{77}$Br]Br-osimertinib is transferred to some organs, and its radioactivity is preserved for an extended time. In the biodistribution study toward tumor-bearing mice, the H1975 tumor accumulation of [$^{77}$Br]Br-osimertinib was extremely dominating compared to that in blood and muscle. Although the radiotracer accumulation in the H1975 tumor was higher than that of blood and muscle, the uptake of this radiotracer was higher in the H3255 tumor compared to H1975 at 4 and 24 h post-injection (Table 6). These findings suggest that the nonspecific accumulation of radiotracers in the H3255 xenograft is greater than in the H1975 xenograft. Furthermore, [$^{77}$Br]Br-osimertinib accumulations in the lung were substantially greater than in the tumor. As a result, in clinical practice, the visibility of tumors in NSCLC patients must be hampered [36].

**Table 6.** Assessment of [$^{77}$Br]Br-osimertinib radiotracer accumulation

| Cell line | EGFR status | Biodistribution (%ID/g) | | |
|---|---|---|---|---|
| | | 1 h | 4 h | 24 h |
| H441 | Wild-type | - | - | - |
| H3255 | Active mutant L858R | 2.68 ± 0.64 | 3.42 ± 0.05 | 2.00 ± 0.59 |
| H1975 | Dual mutation L858R/T790M | 2.73 ± 0.32 | 1.96 ± 0.33 | 0.86 ± 0.14 |

## 3. Discussion

In this study, we have outlined a few of the most important findings about small molecules that have been produced as radiotracers for the imaging of dual mutant EGFR. Most studies in this review evaluated tracers based on their capacity to discriminate cancers based on EGFR expression or mutational status. Some cell lines have been utilized for either purpose in multiple investigations. The L858R/T790M EGFR mutation-expressing H1975 cell line is the only one employed as an indicator for effective dual mutation EGFR targeting. This cell line's accumulation was compared to those of active mutant L858R and/or wild-type EGFR cell lines.

All studies have included blocking experiments to demonstrate the tracer's specificity. Self-blocking has become a prevalent method. However, this is an unfavorable strategy as any affinity for another kinase will not be demonstrated by self-blocking, as the cold compound will also block these off-target receptors [45]. Therefore, it is recommended to utilize a different TKI to inhibit the EGFR in order to reduce the possibility of the compound occupying the same off-target kinases.

Mice are most often used to test small molecule radiotracers preclinically. In the ex vivo biodistribution of [$^{125}$I]ICO1686, a substantial difference in radioactivity concentration was found between male ddY mice and female BALB/C nu/nu mice. Whether this was attributable to mouse strain or sex wasn't discussed. As sex can affect the pharmacokinetics, metabolism, and bioavailability of xenobiotics, it's important for studies to take this into account [46].

## 4. Conclusions

Some radiolabeled imaging probes for EGFR L858R/T790M double mutations were discovered, including [$^{18}$F]FEWZ, [$^{125}$I]ICO1686, [$^{77}$Br]BrCO1686, [$^{125}$I]I-osimertinib, and [$^{77}$Br]Br-osimertinib. These radiolabeled probes were developed based on the third-generation EGFR-TKIs with fundamental evaluations such as *in vitro* and *in vivo* evaluations. Our finding showed that these radiolabeled probes exhibited preference accumulation toward double mutation EGFR L858R/T790M compared to wild-type. However, the summary report states that these probes must be structurally modified to increase the imaging contrast for clinical studies.

## Funding

This work was supported by the Ministry of Research, Technology and Higher Education through the LP2S Universitas Muslim Indonesia, with grant number 161/E5/PG.02.00.PT/2022; 234.h/B.07/UMI/VII/2022.

## Acknowledgments

The authors acknowledge the Faculty of Pharmacy and LP2S Universitas Muslim Indonesia for their support and encouragement in carrying out this research.

## Conflicts of Interest

The authors declare no conflict of interest.

## References


1. Singh, M.; Jadhav, H. R. Targeting non-small cell lung cancer with small-molecule EGFR tyrosine kinase inhibitors. *Drug Discovery Today* **2018,** *23*, 745-753, https://doi.org/10.1016/j.drudis.2017.10.004.
2. Mitsudomi, T.; Morita, S.; Yatabe, Y.; Negoro, S.; Okamoto, I.; Tsurutani, J.; Seto, T.; Satouchi, M.; Tada, H.; Hirashima, T.; Asami, K.; Katakami, N.; Takada, M.; Yoshioka, H.; Shibata, K.; Kudoh, S.; Shimizu, E.; Saito, H.; Toyooka, S.; Nakagawa, K.; Fukuoka, M. Gefitinib versus cisplatin plus docetaxel in patients with non-small-cell lung cancer harbouring mutations of the epidermal growth factor receptor (WJTOG3405): an open label, randomised phase 3 trial. *Lancet Oncol* **2010,** *11*, 121-8, https://doi.org/10.1016/s1470-2045(09)70364-x.
3. Park, S.; Lee, S. Y.; Kim, D.; Sim, Y. S.; Ryu, J.-S.; Choi, J.; Lee, S. H.; Ryu, Y. J.; Lee, J. H.; Chang, J. H., Comparison of epidermal growth factor receptor tyrosine kinase inhibitors for patients with lung adenocarcinoma harboring different epidermal growth factor receptor mutation types. *BMC Cancer* **2021,** *21*, 52, https://doi.org/10.1186/s12885-020-07765-6.
4. Yan, X.-E.; Zhu, S.-J.; Liang, L.; Zhao, P.; Geun Choi, H.; Yun, C.-H., Structural basis of mutant-selectivity and drug-resistance related to CO-1686. *Oncotarget* **2017,** *8*, https://www.oncotarget.com/article/18588/text/.
5. Park, S.; Ha, S.; Lee, S. H.; Paeng, J. C.; Keam, B.; Kim, T. M.; Kim, D. W.; Heo, D. S. Intratumoral heterogeneity characterized by pretreatment PET in non-small cell lung cancer patients predicts progression-free survival on EGFR tyrosine kinase inhibitor. *PLoS One* **2018,** *13*, e0189766, https://doi.org/10.1371/journal.pone.0189766.
6. Araki, T.; Yashima, H.; Shimizu, K.; Aomori, T.; Hashita, T.; Kaira, K.; Nakamura, T.; Yamamoto, K. Review of the treatment of non-small cell lung cancer with gefitinib. *Clin Med Insights Oncol* **2012,** *6*, 407-21, https://doi.org/10.4137/cmo.S7340.
7. Ariyama, T.; Kanno, Y.; Takizawa, S.; Nemoto, K.; Ishii, T. Comparative Study of Different Epidermal Growth Factor Receptor (EGFR)-Tyrosine Kinase Inhibitors Affecting Lung Cancer Cell Lines Stably Overexpressing EGFR Mutations. *BPB Reports* **2021,** *4* , 12-16, https://doi.org/10.1248/bpbreports.4.1_12.
8. Pao, W.; Wang, T. Y.; Riely, G. J.; Miller, V. A.; Pan, Q.; Ladanyi, M.; Zakowski, M. F.; Heelan, R. T.; Kris, M. G.; Varmus, H. E. KRAS Mutations and Primary Resistance of Lung Adenocarcinomas to Gefitinib or Erlotinib. *PLOS Medicine* **2005,** *2* , e17, https://doi.org/10.1371/journal.pmed.0020017.
9. Takeda, M.; Nakagawa, K., First- and Second-Generation EGFR-TKIs Are All Replaced to Osimertinib in Chemo-Naive EGFR Mutation-Positive Non-Small Cell Lung Cancer? *Int J Mol Sci* **2019,** *20*, https://doi.org/10.3390/ijms20010146.
10. Yu, D.; Zhao, W.; Vallega, K. A.; Sun, S. Y., Managing Acquired Resistance to Third-Generation EGFR Tyrosine Kinase Inhibitors Through Co-Targeting MEK/ERK Signaling. *Lung Cancer (Auckl)* **2021,** *12*, 1-10, https://doi.org/10.2147/lctt.S293902.
11. Shi, K.; Wang, G.; Pei, J.; Zhang, J.; Wang, J.; Ouyang, L.; Wang, Y.; Li, W. Emerging strategies to overcome resistance to third-generation EGFR inhibitors. *Journal of Hematology & Oncology* **2022,** *15*, 94, https://doi.org/10.1186/s13045-022-01311-6.
12. Remon, J.; Steuer, C. E.; Ramalingam, S. S.; Felip, E. Osimertinib and other third-generation EGFR TKI in EGFR-mutant NSCLC patients. *Annals of Oncology* **2018,** *29*, i20-i27, https://doi.org/10.1093/annonc/mdx704
13. Kim, E. S. Olmutinib: First Global Approval. *Drugs* **2016,** *76* , 1153-7, https://doi.org/10.1007/s40265-016-0606-z.
14. Nagasaka, M.; Zhu, V. W.; Lim, S. M.; Greco, M.; Wu, F.; Ou, S.-H. I. Beyond Osimertinib: The Development of Third-Generation EGFR Tyrosine Kinase Inhibitors For Advanced EGFR NSCLC. *Journal of Thoracic Oncology* **2021,** *16* , 740-763, https://doi.org/10.1016/j.jtho.2020.11.028.
15. Wu, C. P.; Hung, T. H.; Lusvarghi, S.; Chu, Y. H.; Hsiao, S. H.; Huang, Y. H.; Chang, Y. T.; Ambudkar, S. V. The third-generation EGFR inhibitor almonertinib (HS-10296) resensitizes ABCB1-overexpressing multidrug-resistant cancer cells to chemotherapeutic drugs. *Biochem Pharmacol* **2021,** *188*, 114516, https://doi.org/10.1016/j.bcp.2021.114516.
16. Fawwaz, M.; Mishiro, K.; Nishii, R.; Sawazaki, I.; Shiba, K.; Kinuya, S.; Ogawa, K. Synthesis and Fundamental Evaluation of Radioiodinated Rociletinib (CO-1686) as a Probe to Lung Cancer with L858R/T790M Mutations of Epidermal Growth Factor Receptor (EGFR). *Molecules* **2020,** *25*, 2914, https://doi.org/10.3390/molecules25122914.
17. Hu, L.; Ru, K.; Zhang, L.; Huang, Y.; Zhu, X.; Liu, H.; Zetterberg, A.; Cheng, T.; Miao, W. Fluorescence *in situ* hybridization (FISH): an increasingly demanded tool for biomarker research and personalized medicine. *Biomark Res* **2014,** *2*, 3, https://doi.org/10.1186/2050-7771-2-3.

18. Martinez, P.; Hernández-Losa, J.; Ma Ángeles, M.; Cedrés, S.; Castellví, J.; Martinez-Marti, A.; Tallada, N.; Murtra-Garrell, N.; Navarro-Mendivill, A.; Rodriguez-Freixinos, V.; Canela, M.; Ramon y Cajal, S.; Felip, E. Fluorescence *In situ* Hybridization and Immunohistochemistry as Diagnostic Methods for ALK Positive Non-Small Cell Lung Cancer Patients. *PLOS ONE* **2013,** *8*, e52261, https://doi.org/10.1371/journal.pone.0052261.
19. Lone, S. N.; Nisar, S.; Masoodi, T.; Singh, M.; Rizwan, A.; Hashem, S.; El-Rifai, W.; Bedognetti, D.; Batra, S. K.; Haris, M.; Bhat, A. A.; Macha, M. A., Liquid biopsy: a step closer to transform diagnosis, prognosis and future of cancer treatments. *Molecular Cancer* **2022,** *21*, 79, https://doi.org/10.1186/s12943-022-01543-7.
20. Kang, S.; Woo, J.; Kim, S. A Systematic Review of Companion Diagnostic Tests by Immunohistochemistry for the Screening of Alectinib-Treated Patients in ALK-Positive Non-Small Cell Lung Cancer. *Diagnostics (Basel)* **2022,** *12*, 1297, https://doi.org/10.3390/diagnostics12051297.
21. Lüönd, F.; Tiede, S.; Christofori, G., Breast cancer as an example of tumour heterogeneity and tumour cell plasticity during malignant progression. *British Journal of Cancer* **2021,** *125*, 164-175, https://doi.org/10.1038/s41416-021-01328-7.
22. Xu, G.; Wu, H.; Xu, Y.; Zhang, Y.; Lin, F.; Baklaushev, V. P.; Chekhonin, V. P.; Peltzer, K.; Wang, X.; Mao, M.; Wang, G.; Cui, P.; Zhang, C. Homogenous and Heterogenous Prognostic Factors for Patients with Bone Sarcoma. *Orthopaedic Surgery* **2021,** *13*, 134-144, https://doi.org/10.1111/os.12851.
23. Xiao, Z.; Song, Y.; Kai, W.; Sun, X.; Shen, B., Evaluation of 99mTc-HYNIC-MPG as a novel SPECT radiotracer to detect EGFR-activating mutations in NSCLC. *Oncotarget* **2017,** *8*, 40732-40740, https://doi.org/10.18632/oncotarget.17251.
24. Hirsch, F. R.; Varella-Garcia, M.; McCoy, J.; West, H.; Xavier, A. C.; Gumerlock, P.; Bunn, P. A.; Franklin, W. A.; Crowley, J.; Gandara, D. R. Increased Epidermal Growth Factor Receptor Gene Copy Number Detected by Fluorescence *In situ* Hybridization Associates With Increased Sensitivity to Gefitinib in Patients With Bronchioloalveolar Carcinoma Subtypes: A Southwest Oncology Group Study. *Journal of Clinical Oncology* **2005,** *23*, 6838-6845, https://doi.org/10.1200/jco.2005.01.2823.
25. Ogawa, K.; Masuda, R.; Mizuno, Y.; Makino, A.; Kozaka, T.; Kitamura, Y.; Kiyono, Y.; Shiba, K.; Odani, A. Development of a novel radiobromine-labeled sigma-1 receptor imaging probe. *Nucl Med Biol* **2018,** *61*, 28-35, https://doi.org/10.1016/j.nucmedbio.2018.03.005.
26. Ogawa, K.; Ishizaki, A.; Takai, K.; Kitamura, Y.; Kiwada, T.; Shiba, K.; Odani, A. Development of Novel Radiogallium-Labeled Bone Imaging Agents Using Oligo-Aspartic Acid Peptides as Carriers. *PLOS ONE* **2014,** *8*, e84335, https://doi.org/10.1371/journal.pone.0084335.
27. Rinne, S. S.; Orlova, A.; Tolmachev, V. PET and SPECT Imaging of the EGFR Family (RTK Class I) in Oncology. *Int J Mol Sci* **2021,** *22* , 3663, https://doi.org/10.3390/ijms22073663.
28. Xu, J.; Cai, F.; Geng, C.; Wang, Z.; Tang, X. Diagnostic Performance of CMR, SPECT, and PET Imaging for the Identification of Coronary Artery Disease: A Meta-Analysis. *Frontiers in Cardiovascular Medicine* **2021,** *8*. https://doi.org/10.3389/fcvm.2021.621389.
29. Fass, L., Imaging and cancer: a review. *Mol Oncol* **2008,** *2*, 115-52, https://doi.org/10.1016/j.molonc.2008.04.001.
30. Takeuchi, S.; Zhao, S.; Kuge, Y.; Zhao, Y.; Nishijima, K.-I.; Hatano, T.; Shimizu, Y.; Kinoshita, I.; Tamaki, N.; Dosaka-Akita, H., 18F-Fluorothymidine PET/CT as an early predictor of tumor response to treatment with cetuximab in human lung cancer xenografts. *Oncol Rep* **2011,** *26*, 725-730. https://doi.org/10.3892/or.2011.1338.
31. Song, Y.; Xiao, Z.; Wang, K.; Wang, X.; Zhang, C.; Fang, F.; Sun, X.; Shen, B., Development and Evaluation of 18F-IRS for Molecular Imaging Mutant EGF Receptors in NSCLC. *Scientific Reports* **2017,** *7*, 3121, https://doi.org/10.1038/s41598-017-01443-7.
32. Crișan, G.; Moldovean-Cioroianu, N. S.; Timaru, D. G.; Andrieș, G.; Căinap, C.; Chiș, V., Radiopharmaceuticals for PET and SPECT Imaging: A Literature Review over the Last Decade. *Int J Mol Sci* **2022,** *23*, 5023, https://doi.org/10.3390/ijms23095023.
33. Uenomachi, M.; Takahashi, M.; Shimazoe, K.; Takahashi, H.; Kamada, K.; Orita, T.; Ogane, K.; Tsuji, A. B. Simultaneous *in vivo* imaging with PET and SPECT tracers using a Compton-PET hybrid camera. *Scientific Reports* **2021,** *11*, 17933, https://doi.org/10.1038/s41598-021-97302-7.
34. Goggi, J. L.; Haslop, A.; Ramasamy, B.; Cheng, P.; Jiang, L.; Soh, V.; Robins, E. G. Identifying nonsmall-cell lung tumours bearing the T790M EGFR TKI resistance mutation using PET imaging. *J Labelled Comp Radiopharm* **2019,** *62*, 596-603, https://doi.org/10.1002/jlcr.3771.
35. Fawwaz, M.; Mishiro, K.; Nishii, R.; Makino, A.; Kiyono, Y.; Shiba, K.; Kinuya, S.; Ogawa, K. A Radiobrominated Tyrosine Kinase Inhibitor for EGFR with L858R/T790M Mutations in Lung Carcinoma. *Pharmaceuticals (Basel)* **2021,** *14*, 256, https://doi.org/10.3390/ph14030256.
36. Mishiro, K.; Nishii, R.; Sawazaki, I.; Sofuku, T.; Fuchigami, T.; Sudo, H.; Effendi, N.; Makino, A.; Kiyono, Y.; Shiba, K.; Taki, J.; Kinuya, S.; Ogawa, K. Development of Radiohalogenated Osimertinib Derivatives as Imaging Probes for Companion Diagnostics of Osimertinib. *Journal of Medicinal Chemistry* **2022,** *65* , 1835-1847, https://doi.org/10.1021/acs.jmedchem.1c01211.

37. Cross, D. A.; Ashton, S. E.; Ghiorghiu, S.; Eberlein, C.; Nebhan, C. A.; Spitzler, P. J.; Orme, J. P.; Finlay, M. R.; Ward, R. A.; Mellor, M. J.; Hughes, G.; Rahi, A.; Jacobs, V. N.; Red Brewer, M.; Ichihara, E.; Sun, J.; Jin, H.; Ballard, P.; Al-Kadhimi, K.; Rowlinson, R.; Klinowska, T.; Richmond, G. H.; Cantarini, M.; Kim, D. W.; Ranson, M. R.; Pao, W. AZD9291, an irreversible EGFR TKI, overcomes T790M-mediated resistance to EGFR inhibitors in lung cancer. *Cancer Discov* **2014,** *4*, 1046-61, https://doi.org/10.1158/2159-8290.Cd-14-0337.
38. Robichaux, J. P.; Le, X.; Vijayan, R. S. K.; Hicks, J. K.; Heeke, S.; Elamin, Y. Y.; Lin, H. Y.; Udagawa, H.; Skoulidis, F.; Tran, H.; Varghese, S.; He, J.; Zhang, F.; Nilsson, M. B.; Hu, L.; Poteete, A.; Rinsurongkawong, W.; Zhang, X.; Ren, C.; Liu, X.; Hong, L.; Zhang, J.; Diao, L.; Madison, R.; Schrock, A. B.; Saam, J.; Raymond, V.; Fang, B.; Wang, J.; Ha, M. J.; Cross, J. B.; Gray, J. E.; Heymach, J. V. Structure-based classification predicts drug response in EGFR-mutant NSCLC. *Nature* **2021,** *597*, 732-737, https://doi.org/10.1038/s41586-021-03898-1.
39. Wang, S.; Cang, S.; Liu, D. Third-generation inhibitors targeting EGFR T790M mutation in advanced non-small cell lung cancer. *J Hematol Oncol* **2016,** *9*, 34, https://doi.org/10.1186/s13045-016-0268-z.
40. Walter, A. O.; Sjin, R. T.; Haringsma, H. J.; Ohashi, K.; Sun, J.; Lee, K.; Dubrovskiy, A.; Labenski, M.; Zhu, Z.; Wang, Z.; Sheets, M.; St Martin, T.; Karp, R.; van Kalken, D.; Chaturvedi, P.; Niu, D.; Nacht, M.; Petter, R. C.; Westlin, W.; Lin, K.; Jaw-Tsai, S.; Raponi, M.; Van Dyke, T.; Etter, J.; Weaver, Z.; Pao, W.; Singh, J.; Simmons, A. D.; Harding, T. C.; Allen, A. Discovery of a mutant-selective covalent inhibitor of EGFR that overcomes T790M-mediated resistance in NSCLC. *Cancer Discov* **2013,** *3*, 1404-15, https://doi.org/10.1158/2159-8290.Cd-13-0314.
41. Lu, X.; Yu, L.; Zhang, Z.; Ren, X.; Smaill, J. B.; Ding, K. Targeting EGFRL858R/T790M and EGFRL858R/T790M/C797S resistance mutations in NSCLC: Current developments in medicinal chemistry. *Medicinal Research Reviews* **2018,** *38*, 1550-1581, https://doi.org/10.1002/med.21488.
42. Zhu, L.; Zou, C.; Zhang, Z.; Wang, J.; Yang, L.; Rao, C.; Yang, Z.; Liang, J.; Xia, B.; Shenglin, M. A. Thoracic radiotherapy and concurrent almonertinib for unresectable stage III EGFR-mutated non-small-cell lung cancer: a phase 2 study. *BMC Cancer* **2021,** *21*, 511, https://doi.org/10.1186/s12885-021-08266-w.
43. Ballard, P.; Yates, J. W. T.; Yang, Z.; Kim, D.-W.; Yang, J. C.-H.; Cantarini, M.; Pickup, K.; Jordan, A.; Hickey, M.; Grist, M.; Box, M.; Johnström, P.; Varnäs, K.; Malmquist, J.; Thress, K. S.; Jänne, P. A.; Cross, D. Preclinical Comparison of Osimertinib with Other EGFR-TKIs in EGFR-Mutant NSCLC Brain Metastases Models, and Early Evidence of Clinical Brain Metastases Activity. *Clinical Cancer Research* **2016,** *22*, 5130-5140, https://doi.org/10.1158/1078-0432.CCR-16-0399.
44. Zhou, W.; Ercan, D.; Chen, L.; Yun, C. H.; Li, D.; Capelletti, M.; Cortot, A. B.; Chirieac, L.; Iacob, R. E.; Padera, R.; Engen, J. R.; Wong, K. K.; Eck, M. J.; Gray, N. S.; Jänne, P. A. Novel mutant-selective EGFR kinase inhibitors against EGFR T790M. *Nature* **2009,** *462*, 1070-4, https://doi.org/10.1038/nature08622.
45. Högnäsbacka, A.; Poot, A.J.; Vugts, D.J.; van Dongen, G.A.M.S.; Windhorst, A.D. The Development of Positron Emission Tomography Tracers for In Vivo Targeting the Kinase Domain of the Epidermal Growth Factor Receptor. *Pharmaceuticals* **2022**, *15*, 450. https://doi.org/10.3390/ ph15040450.
46. Hildebrandt, I. J.; Su, H.; Weber, W. A. Anesthesia and Other Considerations for in Vivo Imaging of Small Animals. *ILARJ* **2008**, *49*, 17–26, https://doi.org/10.1093/ilar.49.1.17.